Countering self-protection interrupted sampling repeater jammer against chirp radar

Samer Baher Safa Hanbali [ID]

Department of Communication Engineering, Higher Institute for Applied Science and Technology, Damascus, Syria

Abstract

Interrupted sampling repeater jammer generates multiple false targets to confuse chirp radar systems. In practical situations, maintaining separation between true target echo and jamming signal is not possible because the jamming pulses and the true target echo are overlapping in both time and frequency domains. A new anti-jamming technique against interrupted sampling jamming of self-protection repeater jammer is proposed without the knowledge of the jamming parameters. The proposed technique is based on fractional Fourier transform that can separate the overlapping true target echo and jamming pulses in the fractional domain, and then the resulting pulses are returned to the time domain, the true target can be easily distinguished from the false ones because the jamming pulses lag behind the true target echo by the jammer's delay. The theoretical analysis and simulation results demonstrate the efficiency and validity of the proposed technique.

Introduction

Chirp waveform has high Doppler tolerance. This makes it attractive to be used in radar systems. But different types of deceptive jammers for example interrupted sampling repeater jammer (ISRJ), digital radio frequency memory (DRFM), frequency shifting jammer, and active echo cancelation (AEC) jammer can jam chirp radars and generate false targets or suppress the true target echo [1, 2]. DRFM is commonly used in electronic countermeasure because it can intercept, store, and retransmit jamming signal that are coherent with the radar signal. This makes DRFM jammer benefits from the processing gain of pulse compression and coherent integration. Therefore, DRFM jammer needs low transmitting power to form false targets in the victim radar. DRFM jammers work in two modes [3–7], i.e. full pulse repeating mode and interrupted sampling repeating mode. When DRFM jammer works in full pulse repeating mode, it intercepts, stores, and retransmits the complete radar pulse. But, the jammer pulse lags behind the true target pulse. Therefore, orthogonal waveforms technique can be used to counter DRFM jammer easily [2]. While in interrupted sampling repeating mode, the jammer samples and stores segments of the radar pulse during the radar pulse itself and retransmits them toward the victim radar. This means that the ISRJ signal can be generated in the current radar pulse repetition period, which makes countering techniques such as phase perturbation [8], modifying the chirp rate [9], and pulse diversity [10–13] fail. ISRJ can work under a relatively low transmitting power because it obtains partial processing gain from pulse compression and coherent integration. Therefore, ISRJ generates multiple false targets while the amplitudes of the high-order false targets decrease quickly [6]. The power and the distribution of the false targets can be changed by adjusting the jamming parameters easily. Therefore, ISRJ is superior to other jamming methods. Under certain conditions including the repeater power, delayed time, and repeater frequency, the false target will coincide with the true target for partial echo cancellation [14, 15]. In [16, 17] anti-jamming techniques are presented to eliminate the effect of this kind of AEC.

There is only limited public research literature on electronic counter countermeasure schemes against ISRJ. In [18–21], different methods are proposed to counter ISRJ based on the time-frequency (TF) analysis, where it was found that the TF characteristics of the ISRJ signal are discontinuous. Therefore, a band-pass filter (BPF) can be designed to retain the true target signal and suppress the ISRJ signal. In [22], ISRJ suppression issue is addressed by using TF analysis and target sparse reconstruction. In [23], TF analysis result is used to estimate the jamming parameters of slice number and forwarding times to perform jamming suppression. In general, short-time Fourier transform (STFT) is applied to perform the TF analysis. Therefore, the previous methods in [18–23] are only effective under high signal to noise ratio (SNR). In [24] an anti-jamming method based on designing complementary sequences and receiving filters is proposed. Although that method reduces the influence of the ISRJ on radar detection, but it requires complex optimization design. In [25], an adaptive transmitting scheme based on the jamming parameter estimation is used for ISRJ suppression. But, the jamming suppression performance depends on the accuracy of jamming parameters

estimation. In [26], the radar return filtering is achieved by transforming it into the fractional domain and designing a narrow BPF to suppress jamming signal. The center of the BPF can be set according to the true target peak position in the fractional domain. But the performance of this method is affected by the bandwidth of the BPF. In addition, the true target peak position in the fractional domain cannot be easily calculated because the true target is masked by false targets in the time domain.

Based on the previous discussion, countering ISRJ jamming requires more research in order to overcome the limitations of the mentioned anti-jamming methods. In this paper, we propose a new anti-jamming method for countering ISRJ effectively. The proposed method used fractional Fourier transform (FrFT) to compress and separate overlapping the true target echo and the jamming pulses in the fractional domain. Then, the resulting compressed pulses are transformed to the time domain to compare the pulses' arriving time, the leading pulse will be considered as the true target echo because jamming pulses always lag behind the true target echo by the jammer's delay.

The article is organized as follows. Section "Overview of ISRJ" presents a short overview of ISRJ. In the Section "Chirp pulse compression using FrFT," the chirp pulse compression using FrFT is given. In the Section "The proposed anti-jamming technique," the proposed anti-jamming technique is introduced. Finally, Matlab simulation results are demonstrated in the Section "Simulation and results."

Overview of ISRJ

The authors in [6] proposed interrupted sampling technique which samples segments of radar pulse and retransmits them using a time-sharing single receive–transmit antenna toward the victim radar. In this way, the ISRJ generates a main false target that always lags behind the true target by a jammer's delay τ_d, and multiple false targets that are located around the main false target. ISRJ has many advantages because it used a single time-sharing antenna that has easy implementation and therefore it can be carried by a missile. In addition, ISRJ generates multiple false targets without sampling and retransmitting the whole radar pulse.

Let $x(t)$ be the complex representation of the transmitted radar chirp:

$$x(t) = rect\left(\frac{t}{T}\right)e^{j\mu\pi t^2} \qquad (1)$$

where $\mu = B/T$ is the frequency modulation slope, T is the chirp duration, and B is the sweep bandwidth.

The sampling function $p(t)$ is a rectangular pulse train with a pulse duration τ and pulse repeat interval T_s. $p(t)$ can be written as:

$$p(t) = rect\left(\frac{t}{\tau}\right)\sum_{n=-\infty}^{\infty}\delta(t - nT_s) \qquad (2)$$

where $rect(t/\tau)$ represents a rectangular pulse of width τ. The sampled jamming signal is [6]:

$$x_s = p(t) \cdot x(t) \qquad (3)$$

The spectrum of the sampled jamming signal is [6]:

$$X_s(f) = \sum_{n=-\infty}^{\infty} a_n X(f - nf_s) \qquad (4)$$

where $a_n = \tau f_s\mathrm{sinc}(\pi nf_s\tau)$, $f_s = 1/T_s$ is the sampling frequency of ISRJ, and τ is the sampling period of ISRJ. Clearly, $X_s(f)$ is a superposition of the shifted replicas of $X(f)$ scaled by a_n. The output of the radar-matched filter is given as [6]:

$$y(t) = \sum_{n=-\infty}^{\infty} a_n u_n(t) \qquad (5)$$

$$u_n(t) = \mathrm{sinc}[\pi(nf_s + \mu t)(T - |t|)]\left(1 - \frac{|t|}{T}\right)e^{j\pi nf_s t} \qquad (6)$$

where $n = 0, \pm 1, \pm 2, \pm 3\dots$ Based on equations (5) and (6), the output of the radar-matched filter composed of multiple false targets $u_n(t)$, each one has a frequency shift nf_s and a scale factor a_n. The relative distance between each two adjacent false targets equals $cf_s/2\mu$, where c is the propagation speed of light. When the value of n increases, the amplitudes of false targets decrease quickly. Therefore, the ISRJ technique generates about five effective false targets as shown in Fig. 1.

Chirp pulse compression using FrFT

FrFT has been used in sonar and radar signal processing. In [27], a radar-matched filter based on FrFT is implemented for a chirp radar. In [28], the detection and separation of overlapping chirp acoustic signals is achieved by FrFT-based receiver. In [29], an anti-jamming method against frequency shifting jamming is proposed, where FrFT resolves the overlapping jamming pulses and true target echo. Then, the resulting signals are returned to the frequency domain where their spectra are compared with that of the transmitted radar chirp after Doppler compensation. The signal that has less differences of the center frequency is considered as the true target. But, that anti-jamming method cannot counter ISRJ because both the true target and the main false
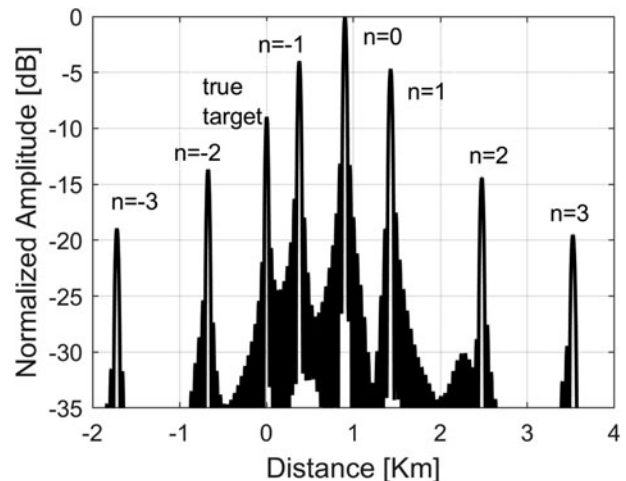

Figure 1. Simulation result of ISRJ.

target have the same frequency shift, and therefore the true target cannot be distinguished from the main false one. In [30], FrFT is used for countering smeared spectrum jamming, where the anti-jamming method benefits from the fact that the jamming pulses have a different frequency modulation slope from that of the transmitted radar chirp. Therefore, the jamming pulses can be suppressed in the fractional domain, and then the true target can be distinguished easily. But, that technique is inefficient in the case of ISRJ because both the true target echo and the jamming pulses have the same frequency modulation slope.

FrFT is a general form of the Fourier transform (FT) that transforms a function into an intermediate domain between frequency and time by rotating the TF plane. If F_α denotes the operator corresponding to the FrFT of angle α, then $F_{\pi/2} = F$: rotation by $\pi/2$ gives FT [31, 32]. In the same way that has been done for standard FT, a sampling theorem for FrFT is proposed in [33]. Compared with FT, the FrFT of optimal angle, α_{opt}, applied to a chirp pulse, concentrates its energy distribution in the fractional domain. This presents the use of the FrFT for pulse compression of chirp pulse [27–30, 34–37]. The continuous FrFT of a signal x (t) is given by [31, 32]:

$$X_\alpha(u) = \int_{-\infty}^{\infty} x(t)K_\alpha(t, u)dt \tag{7}$$

where $K_\alpha(t, u)$ is the transform kernel and when $\alpha \neq n\pi$ it equals [31, 32]:

$$K_\alpha(t, u) = \sqrt{1 - j\cot\alpha}\; e^{j2\pi((t^2+u^2)/2)\cot\alpha - j2\pi ut\csc\alpha} \tag{8}$$

where $\cot\alpha = 1/\tan\alpha$ and $\csc\alpha = 1/\sin\alpha$. Hence:

$$X_\alpha(u) = \int_{-\infty}^{\infty} x(t)\sqrt{1 - j\cot\alpha}\; e^{j2\pi((t^2+u^2)/2)\cot\alpha} \times e^{-j2\pi ut\csc\alpha}dt \tag{9}$$

Applying the FrFT to the chirp pulse given by equation (1) gives:

$$X_\alpha(u) = A_\alpha \int_{-T/2}^{T/2} e^{j\pi t^2(\mu+\cot\alpha) - j2\pi ut\csc\alpha}dt \tag{10}$$

where $A_\alpha = \sqrt{1 - j\cot\alpha}\; e^{j\pi u^2\cot\alpha}$. The integral in this equation involves an error function. But when:

$$\mu + \cot\alpha = 0 \tag{11}$$

Then

$$\alpha = -\text{arccot}(\mu) \tag{12}$$

A condition considered in [37] as being optimal and denoted by α_{opt}, then equation (10) is rewritten as:

$$X_{\alpha opt}(u) = A_\alpha T \frac{\sin\left[\pi(u\csc\alpha_{opt})T\right]}{\pi(u\csc\alpha_{opt})T} \tag{13}$$

Usually, $\mu \gg 1$, so equation (12) gives $\csc\alpha_{opt} = \mu$. Consequently,

$|A_\alpha| = \left|\sqrt{1 - j\cot\alpha_{opt}}\right| = \sqrt{\mu}$. Hence [29]:

$$\left|X_{\alpha opt}(u)\right| = \sqrt{BT}\frac{\sin(\pi Bu)}{\pi Bu} \tag{14}$$

This equation is equivalent to that of the matched filter for chirp pulse. This means that the FrFT compresses chirp pulse like matched filter does [27–30, 34–37]. But, the matched filter is superior to FrFT by 3 dB [36].

The proposed anti-jamming technique

Figure 2 shows the block diagram of the proposed anti-jamming receiver. The jamming signal is a delayed superposition of the shifted replicas of the spectrum of the true target. Consequently, we can discriminate the false targets if we can separate each received pulse in the fractional domain and then return each separated compressed pulse to the time domain to find the leading pulse that will be considered as the true target echo because the jamming pulses lag behind the true target echo by jammer's delay τ_d. After discriminating the true target echo at the output of anti-jamming receiver, the true target can be recognized at the output of the conventional radar receiver based on the start time of the leading pulse. As shown in Fig. 2, $r(t)$ is the baseband received signal that is composed of the sum of the true target echo $x(t - t_0)$, the sampled jamming signal $x_j(t - (t_0 + \tau_d))$, and the noise signal $n(t)$:

$$r(t) = x(t - t_0) + x_j(t - (t_0 + \tau_d)) + n(t) \tag{15}$$

where t_0 is the true target delay. Now, applying the FrFT to the received signal $r(t)$ given by equation (15) gives:

$$F_\alpha(r(t)) = X_\alpha(u - u_0) + C_nX_{j,\alpha}(u - u_1 - w\sin\alpha) + N_\alpha(u) \tag{16}$$

where $w = 2\pi nf_s$, $u_0 = t_0\cos\alpha$, $u_1 = (t_0 + \tau_d)\cos\alpha$, and $F_\alpha(x_s(t)e^{jwt}) = C_nX_{j,\alpha}(u - w\sin\alpha)$. These equations are respectively derived from the delay property and the modulation property of FrFT, where C_n is [31, 32]:

$$C_n = e^{-((jw^2(\sin\alpha\cos\alpha))/2)+juw\cos\alpha} \tag{17}$$

At the optimum value of α given in equation (12) [37], the energy distribution of both the jamming signal and the true target echo concentrate well because these signals have the same frequency modulation slope. Therefore, we get

$$F_{\alpha opt}(r(t)) = \sqrt{BT}\frac{\sin(\pi B(u - u_0))}{\pi B(u - u_0)}$$
$$+ \left\{\sum_{n=-\infty}^{+\infty} C_na_n\sqrt{BT}\frac{\sin[\pi B(u - u_1 - w\sin\alpha_{opt})]}{\pi B(u - u_1 - w\sin\alpha_{opt})}\right\}$$
$$+ N_{\alpha opt}(u) \tag{18}$$

Equation (18) shows that, apart from the noise component $N_\alpha(u)$, the output of the FrFT is composed of sinc functions separated in the fractional domain. After constant false alarm rate (CFAR) detection, the peak position sample and the adjacent samples are kept for each main lobe and the remaining samples are put to zero. This is because most of the energy
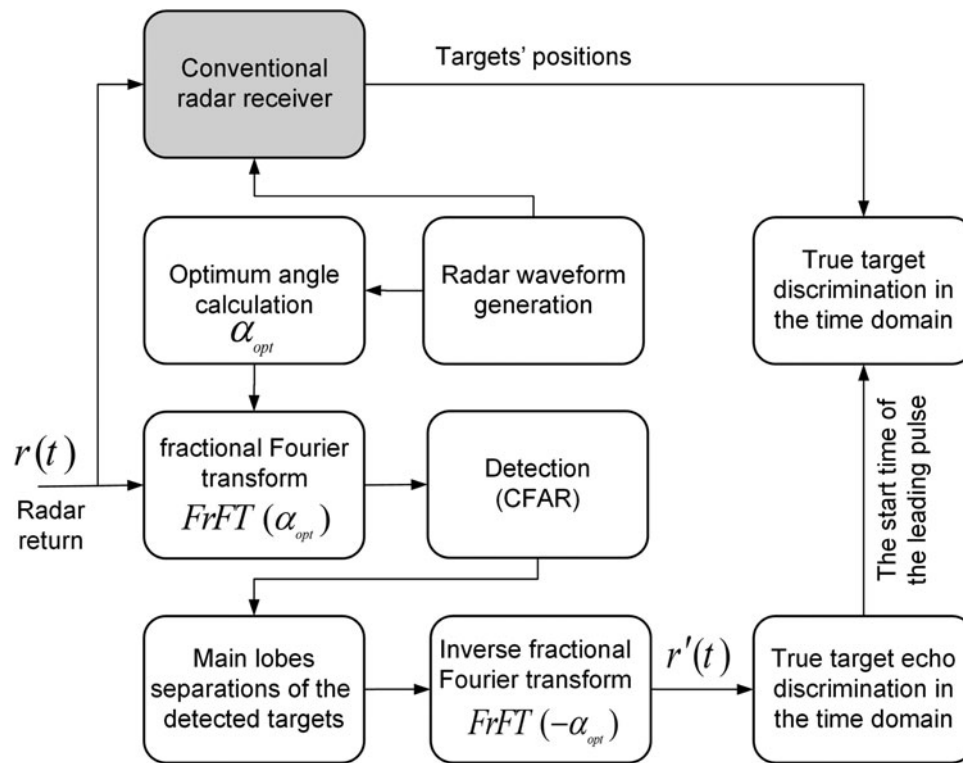
Figure 2. Block diagram of the proposed anti-jamming receiver against ISRJ.

of each jamming pulse is concentrated in its main lobe. As a result, the true target echo and the jamming components are separated and filtered from noise in the fractional domain simultaneously. Then by applying the inverse FrFT, for each main lobe, at $-\alpha_{opt}$, we get

$$r'(t) = x(t - t_0) + \sum_{n=-\infty}^{+\infty} x(t - t_0 - \tau_d) \qquad (19)$$

Equation (19) shows that the output of the inverse FrFT is composed of true target echo and jamming pulses that are delayed replicas of the true target echo and these pulses are separated in the time domain. Now, the true target is discriminated at the output of the conventional radar receiver based on the start time of the leading pulse at the output of the proposed anti-jamming receiver as shown in Fig. 2.

It worth mentioning that α_{opt} is calculated in the discrete domain using equation (20) [27, 28]:

$$\alpha_{opt} = -\tan^{-1}\left(\frac{F_s^2}{\mu L}\right) \qquad (20)$$

where L is the number of samples in the time received window.

The computation complexity of the proposed technique depends on the implementation of FrFT. Since the FrFT can be implemented using FFT, its computational complexity is $O(N\log N)$ [38–40]. As we mentioned above FrFT behaves like a matched filter. In contrast, FrFT requires higher sampling rate than Nyquist frequency [41]. But, this is attainable very easily on current field programmable gate arrays. As a result, the proposed technique is appropriate for practical application.

Simulation and results

Figure 3 shows the assumed simulation scenario for countering self-protection ISRJ, which generates jamming signal from the transmitted radar pulse. In this case, the radar return is the sum of the true target echo and the jamming signal. Then, radar return is received by both the conventional radar receiver and the proposed anti-jamming receiver at the same time. The proposed anti-jamming technique estimates the start time of the true target echo, which leads all jamming pulses in the time domain. Finally, the true target is discriminated by comparing the targets' positions, at the output of the conventional radar receiver, and the start time of the leading pulse at the output of the proposed anti-jamming receiver.

We assume these parameters: $B = 4$ MHz, $T = 100$ μs, sampling frequency, $F_s = 20$ MHz, $L = 14\,000$, and $\alpha_{opt} = -0.6202$ after calculation using equation (20). The true target's delay is 466 μs. The jammer parameters are given as follows: $\tau = 2$ μs, $f_s = 140$ kHz, $\tau_d = 6$ μs, and jamming to signal ratio (JSR) = 16 dB. For simplicity, we assume that the main false target (component of $n = 0$), the false target (component of $n = -1$, the first false target preceding the main false target), the -2nd false target (component of $n = -2$, the second false target preceding the main false target), the $+1$st false target (component of $n = +1$, the first false target lagging behind the main false target), and the $+2$nd false target (component of $n = +2$, the second false target lagging behind the main false target) are detectable, and the other false targets are below the radar detection threshold.

Countering jamming mode a

In this case, the true target leads the -1st order false target and the main false target lags behind the true target, by $\tau_d = 6$ μs as
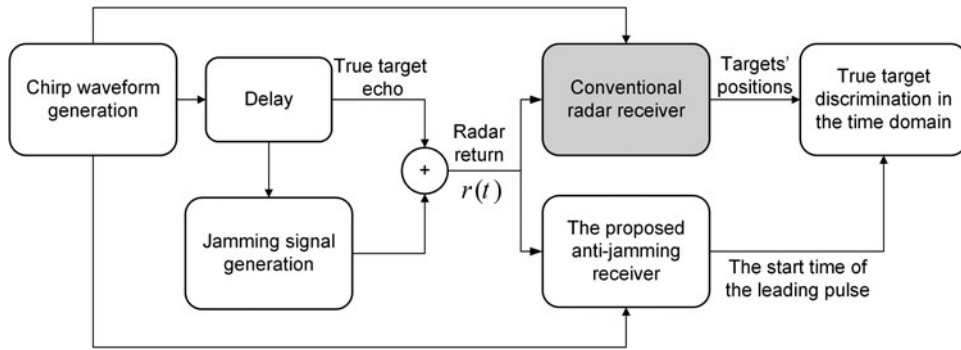
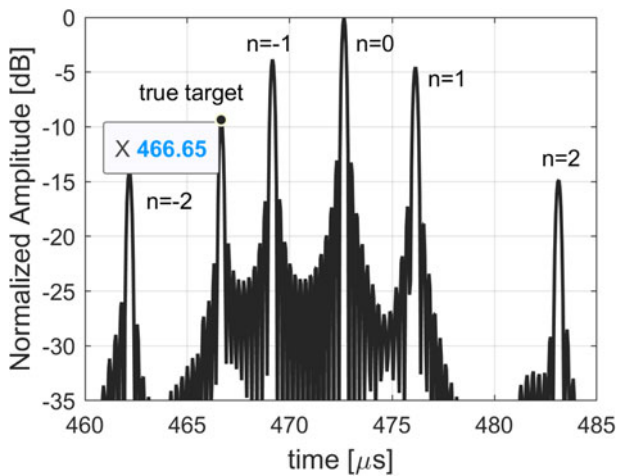**Figure 3.** Simulation scenario for countering self-protection ISRJ.

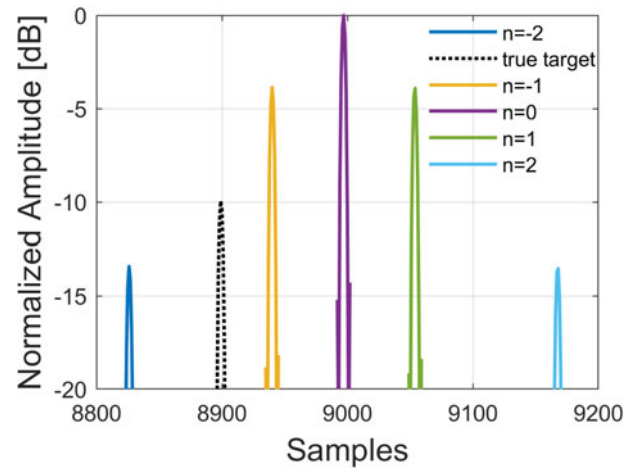**Figure 4.** Matched filter output in the case of ISRJ.

Figure 6. Separation of main lobes in the fractional domain in the case of ISRJ.
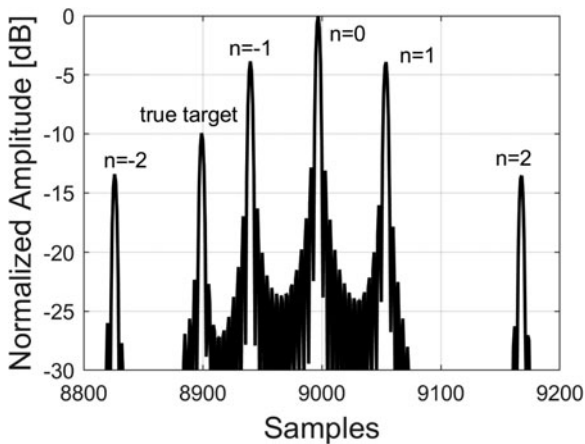

Figure 5. FrFT of the received signal in the case of ISRJ.
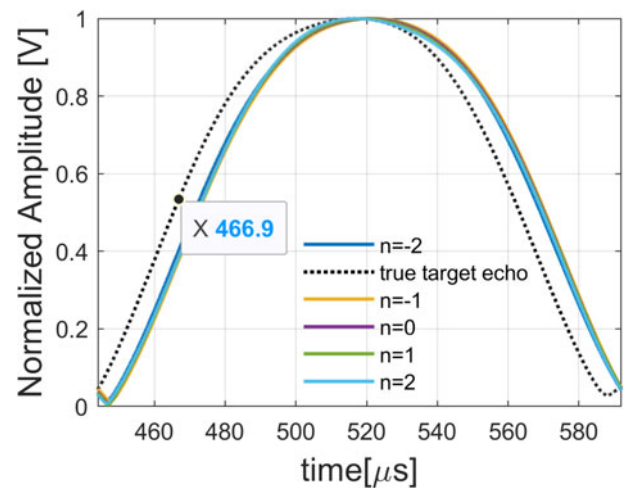

Figure 7. Resulting pulses after returning to the time domain in the case of ISRJ.

shown in Fig. 4. The true target echo and jamming pulses can be separated and isolated easily in different compressed pulses at the output of FrFT as shown in Figs 5 and 6 respectively. Then these compressed pulses are now returned to the time domain to give the independent pluses as shown in Fig. 7, the second pulse leads the other pulses by τ_d. Therefore, the dotted curve belongs to the true target echo and the overlapping solid curves belong to the jamming pulses. Consequently, the second target, at the

output of radar-matched filter, represents the true target that has a delay of 466 µs as shown in Fig. 4.

Countering jamming mode b

To confuse the radar well, the −1st order false target leads the true target when $f_s > \sqrt{B/T}$, e.g. $f_s = 480$ kHz, as shown in Fig. 8. At
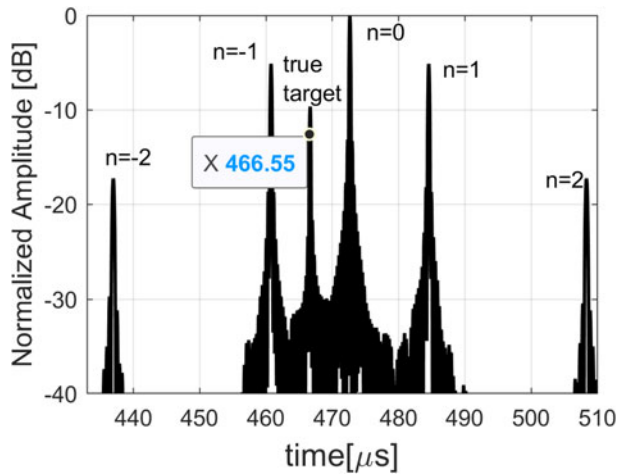
Figure 8. Matched filter output when the first-order false target leads the true target.
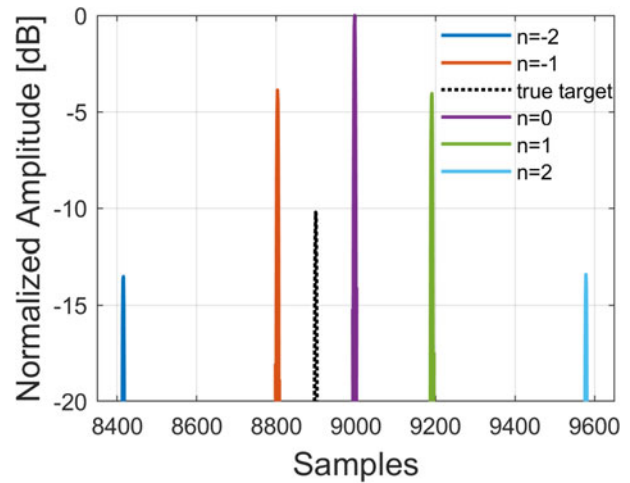

Figure 9. FrFT of the received signal when the first-order false target leads the true target.

Figure 10. Separation of main lobes in the fractional domain when the first-order false target leads the true target.
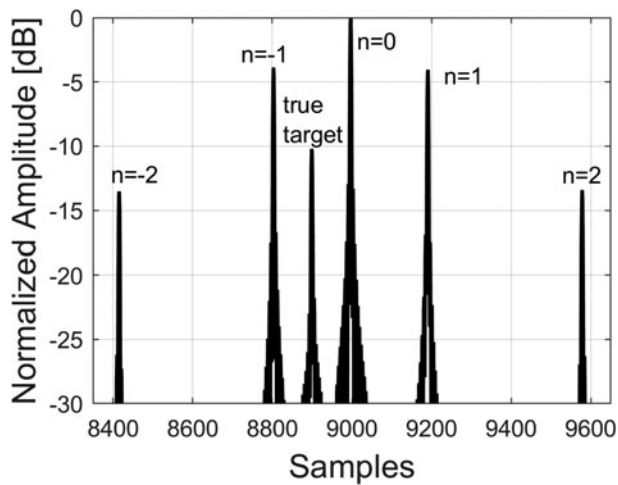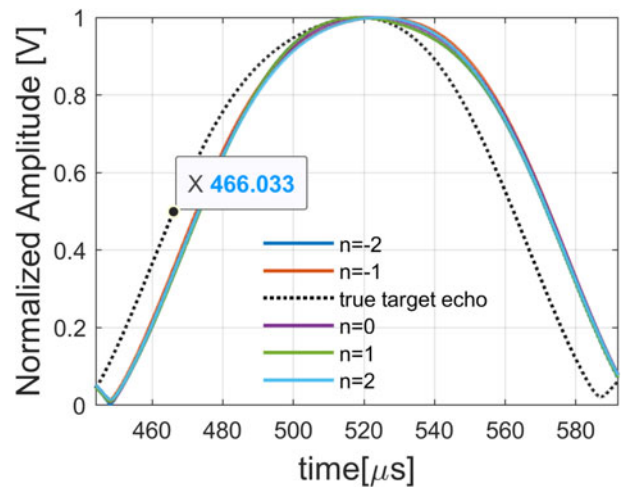

Figure 11. Resulting pulses after returning to the time domain when the first-order false target leads the true target.

the output of FrFT, the jamming pulses and the true target can be separated and isolated easily in different compressed pulses as shown in Figs 9 and 10 respectively. Then these compressed pulses are now returned to the time domain to give the independent pulses shown in Fig. 11, the third pulse leads the other pulses by τ_d. Therefore, the dotted curve belongs to the true target echo and the overlapping solid curves belong to the jamming pulses. Consequently, the third target, at the output of the radar-matched filter, represents the true target that has a delay of 466 μs as shown in Fig. 8.

The performance of the proposed method

Now, we will simulate the probability of detection (P_d) as a function of SNR when the probability of false alarm ($P_{fa} = 10^{-6}$). As shown in Fig. 12, the FrFT is inferior to the matched filter by 3 dB in terms of SNR, but it is superior to STFT. Therefore, the anti-jamming techniques based on STFT require high SNR to be effective [18–23]. However, the proposed method works well under low SNR. This is because FrFT benefits from pulse compression gain. Despite the fact that FrFT requires high sampling rate, the proposed method is superior to other methods.
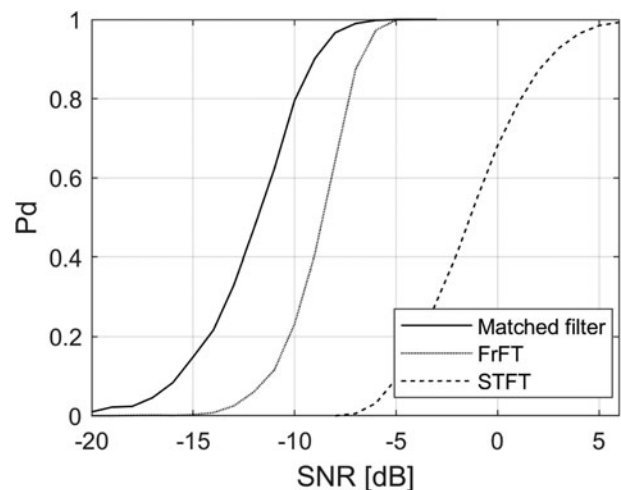

Figure 12. Performance of FrFT versus matched filter and STFT.

It is well known that conventional CFAR masks the weaker of the two closely spaced targets. Therefore, radar systems used modified CFAR such as the censored (CS) CFAR, order statistics (OS) CFAR, and smallest-of cell-averaging (SOCA) CFAR, which are designed to overcome mutual target masking [42]. It worth mentioning that self-protection ISRJ does not transmit high power to avoid hostile anti-radiation missile attack [43]. When high JSR is used, a mutual target masking occurs. Therefore, the proposed anti-jamming receiver used modified CFAR. Consequently, as long as the true target is detected by modified CFAR, the proposed method works well.

Conclusion

Chirp radars are vulnerable to many types of deceptive jammers e.g. ISRJ that generates multiple false targets and makes the radar system unable to discriminate the true target. We proposed a new anti-jamming technique based on FrFT to counter ISRJ jamming, where the true target echo and jamming pulses are compressed and separated in the fractional domain. Then, these separated pulses are returned to the time domain to discriminate the true target echo that leads the jamming pulses by the jammer's delay. Despite the fact that the proposed method is inferior to the matched filter and it requires high sampling rate, it is suitable for practical application. Because, it works better than other anti-jamming techniques that require high SNR or high computational cost or the knowledge of the jamming parameters. This makes it attractive to be incorporated into existing radar systems.

References

1. **Baher Safa Hanbali S** (2018) A review of radar signals in terms of Doppler tolerance, time-sidelobe level, and immunity against jamming. *International Journal of Microwave and Wireless Technologies* **10**, 1134–1142.
2. **Baher Safa Hanbali S and Kastantin R** (2017) A review of self-protection deceptive jamming against chirp radars. *International Journal of Microwave and Wireless Technologies* **9**, 1853–1861.
3. **Greco M, Gini F and Farina A** (2008) Radar detection and classification of jamming signals belonging to a cone class. *IEEE Transactions on Signal Processing* **56**, 1984–1993.
4. **Zhang J, Zhu D and Zhang G** (2013) New antivelocity deception jamming technique using pulses with adaptive initial phases. *IEEE Transactions on Aerospace and Electronic Systems* **49**, 1290–1300.
5. **Lu Y and Li S** (2017) CFAR detection of DRFM deception jamming based on singular spectrum analysis. *IEEE International Conference on Acoustics, Speech, and Signal Processing, Communications and Computing, Xiamen*, IEEE, China, pp. 1–6.
6. **Wang XS, Liu JC, Zhang WM, Fu QX, Liu Z and Xie XX** (2007) Mathematic principles of interrupted-sampling repeater jamming (ISRJ). *Science in China Series F: Information Sciences* **50**, 113–123.
7. **Li C, Su W, Gu H, Ma C and Chen J** (2014) Improved interrupted sampling repeater jamming based on DRFM. *IEEE International Conference on Acoustics, Speech, and Signal Processing, Communications and Computing*, IEEE, Guilin, China, pp. 5–8.
8. **Soumekh M** (2006) SAR-ECCM using phase-perturbed LFM chirp signals and DRFM repeat jammer penalization. *IEEE Transactions on Aerospace and Electronic Systems* **42**, 191–205.
9. **Feng X-Z and Xu X-J** (2009) Study of countermeasures to deceptive jamming using random linear modulation frequency ratio SAR. *Systems Engineering and Electronics* **31**, 69–73.
10. **Akhtar J** (2007) An ECCM signaling approach for deep fading of jamming reflectors. *Proceedings of the IET International Conference on Radar Systems*, IET, Edinburgh, UK, pp. 1–5.
11. **Akhtar J** (2009) Orthogonal block coded ECCM schemes against repeat radar jammers. *IEEE Transactions on Aerospace and Electronic Systems* **45**, 1218–1226.
12. **Schuerger J and Garmatyuk D** (2009) Performance of random OFDM radar signals in deception jamming scenarios. *Proceedings of the IEEE Radar Conference*, IEEE, Pasadena, CA, USA, pp. 1–6.
13. **Zhang JD, Zhu XH and Wang KR** (2009) A waveform diversity technique for countering RGPO. *Proceedings of the IET International Radar Conference*, IET, Guilin, China, pp. 1–4.
14. **Feng DJ, Xu LT, Wang W and Yang H** (2014) Radar echo cancellation using interrupted-sampling repeater. *IEICE Electronics Letters* **11**, 1–6.
15. **Qihua Wu, Zhao F, Wang J, Liu X and Xiao S** (2019) Improved ISRJ-based radar target echo cancellation using frequency shifting modulation. *Electronics* **8**, 1–8.
16. **Baher Safa Hanbali S and Kastantin R** (2017) Technique to counter active echo cancellation of self-protection ISRJ. *IET Electronics Letters* **53**, 680–681.
17. **Baher Safa Hanbali S** (2019) Technique to counter improved active echo cancellation based on ISRJ with frequency shifting. *IEEE Sensors Journal* **19**, 9194–9199.
18. **Gong SX, Wei XZ and Li X** (2014) ECCM scheme against interrupted sampling repeater jammer based on time-frequency analysis. *Journal of Systems Engineering and Electronics* **25**, 996–1003.
19. **Yuan H, Wang C-y., Li X and An L** (2017) A method against interrupted-sampling repeater jamming based on energy function detection and band-pass filtering. *International Journal of Antennas and Propagation* **2017**, 1–9.
20. **Chen J, Wu W, Xu S, Chen Z and Zou J** (2019) Band pass filter design against interrupted-sampling repeater jamming based on time-frequency analysis. *IET Radar, Sonar and Navigation* **13**, 1646–1654.
21. **Xiong W, Zhang G and Liu W** (2017) Efficient filter design against interrupted sampling repeater jamming for wideband radar. *EURASIP Journal on Advances in Signal Processing* **2017**, 1–12.
22. **Wang Z, Li J, Yu W, Luo Y and Yu Z** (2022) A novel interrupted-sampling repeater jamming suppression method based on time-frequency analysis and target sparse reconstruction. *International Journal of Antennas and Propagation* **2022**, 2812456.
23. **Zhou C, Liu Q and Chen X** (2018) Parameter estimation and suppression for DRFM-based interrupted sampling repeater jammer. *IET Radar, Sonar & Navigation* **12**, 56–63.
24. **Wang F, Li N, Pang C, Li C, Li Y and Wang X** (2022) Complementary sequences and receiving filters design for suppressing interrupted sampling repeater jamming. *IEEE Geoscience and Remote Sensing Letters* **19**, 1–5.
25. **Zhou C, Liu F and Liu Q** (2017) An adaptive transmitting scheme for interrupted sampling repeater jamming suppression. *Sensors* **17**, 1–16.
26. **Liua M, Shu T and Chen Q** (2018) Countermeasure for interrupted-sampling repeater jamming based on fractional Fourier transformation. *MATEC Web of Conferences* **232**, 03037.
27. **Elgamel SA and Soraghan JJ** (2010) Radar matched filtering using the fractional Fourier transform. *Sensor Signal Processing for Defence (SSPD 2010)*, IET, London, UK, pp. 1–5.
28. **Cowell D and Freear S** (2010) Separation of overlapping linear frequency modulated (LFM) signals using the fractional Fourier transform. *IEEE Transactions on Ultrasonics, Ferroelectrics, and Frequency Control* **57**, 2324–2333.
29. **Baher Safa Hanbali S and Kastantin R** (2017) Fractional Fourier transform based chirp radars for countering self-protection frequency shifting jammers. *International Journal of Microwave and Wireless Technologies* **9**, 1687–1693.
30. **Baher Safa Hanbali S** (2021) Countering self protection smeared spectrum jamming against chirp radars. *IET Radar, Sonar & Navigation* **15**, 1–8.

31. **Almeida LB** (1994) The fractional Fourier transform and time frequency representations. *IEEE Transactions on Signal Processing* **42**, 3084–3093.

32. **Ashok Narayanana V and Prabhub KMM** (2003) The fractional Fourier transform: theory, implementation and error analysis. *Microprocessors and Microsystems* **27**, 511–521.

33. **Torres R, Pellat-Finet P and Torres Moreno YM** (2004) Sampling theorem in fractional Fourier domains. *5th Iberoamerican Meeting on Optics and 8th Latin American Meeting on Optics, Lasers, and Their Applications*, Vol. 5622, SPIE, Porlamar, Venezuela, pp. 1188–1192.

34. **Sun H-B, Liu G-S, Gu H and Su W-M** (2002) Application of the fractional Fourier transform to moving target detection in airborne SAR. *IEEE Transactions on Aerospace and Electronic Systems* **38**, 1416–1424.

35. **Guoh Y and Guan J** (2010) Detection of moving target based on fractional Fourier transform in SAR clutter. *Signal Processing (ICSP), 2010 IEEE 10th International Conference on*, IEEE, Beijing, China, pp. 2003–2006.

36. **Liu J-C, Liu Z and Wang X-S** (2007) SNR analysis of LFM signal with Gaussian white noise in fractional Fourier transform domain. *Journal of Electronics and Information Technology* **29**, 2337–2340.

37. **Capus C and Brown K** (2003) Short-time fractional Fourier methods for the time-frequency representation of chirp signals. *Journal of the Acoustical Society of America* **113**, 3253–3263.

38. **Ozaktas H, Zalevsky Z and Kutay M** (2001) *The Fractional Fourier Transform: With Applications in Optics and Signal Processing.* Chichester, UK: Wiley, pp. 99–107.

39. **Ozaktas H, Arikan O, Kutay M and Bozdagt G** (1996) Digital computation of the fractional Fourier transform, signal processing. *IEEE Transactions on* **44**, 2141–2150.

40. **Cooley JW and Tukey JW** (1965) An algorithm for the machine calculation of complex Fourier series. *Mathematics of computation* **19**, 297–301.

41. **Sejdic E, Djurovic I and Stankovi LJ** (2011) Fractional Fourier transform as a signal processing tool: an overview of recent developments. *Signal Process* **91**, 189–215.

42. **Richards MA** (2014) *Fundamentals of Radar Signal Processing*, 2nd Edn. New York: McGraw- Hill.

43. **Adamy DL** (2015) EW 104, EW against a New Generation of Threats. 2015. Artech House.

Samer Baher Safa Hanbali earned his B.Sc. in electronic engineering from Damascus University, Syria, in 2000; his M.Sc. in advanced electronic engineering from FH Joanneum University, Austria, in 2011; and his Ph.D. in telecommunications from the Higher Institute for Applied Sciences and Technology (HIAST), Damascus, Syria, in 2017. He is a researcher in the Department of Communication Engineering, HIAST, Damascus, Syria.